



HAL
open science

Calculation of the Distribution of Incoming Solar Radiation in Enclosures

K. Chatziangelidis, D. Bouris

► **To cite this version:**

K. Chatziangelidis, D. Bouris. Calculation of the Distribution of Incoming Solar Radiation in Enclosures. Applied Thermal Engineering, 2010, 29 (5-6), pp.1096. 10.1016/j.applthermaleng.2008.05.026 . hal-00626332

HAL Id: hal-00626332

<https://hal.science/hal-00626332>

Submitted on 26 Sep 2011

HAL is a multi-disciplinary open access archive for the deposit and dissemination of scientific research documents, whether they are published or not. The documents may come from teaching and research institutions in France or abroad, or from public or private research centers.

L'archive ouverte pluridisciplinaire **HAL**, est destinée au dépôt et à la diffusion de documents scientifiques de niveau recherche, publiés ou non, émanant des établissements d'enseignement et de recherche français ou étrangers, des laboratoires publics ou privés.

Accepted Manuscript

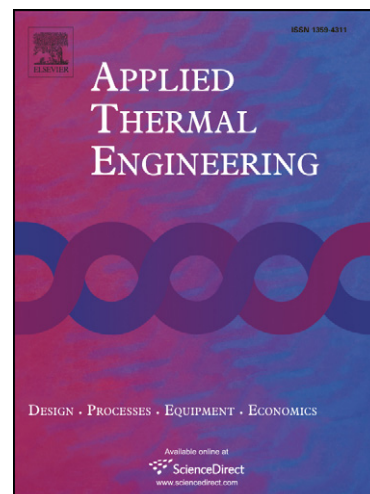
Calculation of the Distribution of Incoming Solar Radiation in Enclosures

K. Chatziangelidis, D. Bouris

PII: S1359-4311(08)00258-5
DOI: [10.1016/j.applthermaleng.2008.05.026](https://doi.org/10.1016/j.applthermaleng.2008.05.026)
Reference: ATE 2528

To appear in: *Applied Thermal Engineering*

Received Date: 19 October 2007
Revised Date: 16 May 2008
Accepted Date: 28 May 2008



Please cite this article as: K. Chatziangelidis, D. Bouris, Calculation of the Distribution of Incoming Solar Radiation in Enclosures, *Applied Thermal Engineering* (2008), doi: [10.1016/j.applthermaleng.2008.05.026](https://doi.org/10.1016/j.applthermaleng.2008.05.026)

This is a PDF file of an unedited manuscript that has been accepted for publication. As a service to our customers we are providing this early version of the manuscript. The manuscript will undergo copyediting, typesetting, and review of the resulting proof before it is published in its final form. Please note that during the production process errors may be discovered which could affect the content, and all legal disclaimers that apply to the journal pertain.

Calculation of the Distribution of Incoming Solar Radiation in Enclosures

K. Chatziangelidis and D. Bouris^(*)

Department of Engineering and Management of Energy Resources

University of Western Macedonia

Bakola & Sialvera, 50100, Kozani, Greece

Abstract

Solar heat gains are an important factor in the calculation of cooling loads for buildings. This paper aims at introducing an improved methodology to calculate the distribution of incoming solar energy on the internal surfaces of closed spaces with multiple openings. The independent numerical methodology is based on the view factor theory and in order to justify and prove its functionality, it has been linked to the commercial software of *TRNSYS*, which normally uses a surface area ratio based algorithm for the same process. For the simplified building structures that have been examined, there are noticeable differences in the spatial and temporal distribution of the absorbed solar energy. The proposed approach is indeed an improvement over the surface area ratio method, having a strong physical basis with relatively little extra computational effort.

Keywords: solar radiation, *TRNSYS*, view factor, enclosure, thermal simulation, thermal comfort

^(*)**Corresponding author**

Tel.: +30 24610 56675, Fax.: +30 24610 56676, Email: dmpouris@uowm.gr

1. Introduction

The need for accurate simulation models, concerning the distribution of solar energy entering domestic buildings has become the main subject of many research efforts in the last few decades. Improved accuracy of the distribution algorithm will lead to more accurate prediction of the energy requirements of the simulated building and therefore valid conclusions regarding energy efficiency and indoor thermal comfort conditions ([1])

Calculation of the distribution of incoming solar energy in enclosed spaces can be accomplished through a number of different approaches with increasing levels of complexity, computational effort and accuracy. Wall [2] has presented an interesting study comparing four such approaches for solar radiation distribution in a room and concluded that a geometrical description of the enclosed space is important and transmission through windows, reflection and absorption must be accurately taken into account. Perhaps the simplest approach is that of an area weighted distribution whereby only the area of each surface (i.e. walls) is used in the distribution algorithm. This is the approach currently applied by the commercial software TRNSYS [3], with a surface absorptance factor also being taken into account but no other geometrical relations between the enclosure surfaces e.g. view factors. The more accurate approach is that of the exact calculation of 'sun patches' that are formed as direct solar radiation passes through windows. However, this requires detailed geometrical information with regard to internal surfaces, the borders of the enclosure's openings and the time varying position of the sun. Athienitis and Stylianou [4] and Cucumo et al. [5], presented analysis for estimating the solar absorptance of a room, based on the radiosity-

irradiation method (RIM) algorithm that was developed by Sparrow and Cess [6]. The above mentioned algorithm (RIM) uses the view factor theory and leads to an $N * N$ system of equations, where N refers to the number of elements that the larger wall surface is divided into. Later on, Wen and Smith [7] developed a model which describes the dynamic thermal behavior of a building, considering its inner space to be surrounded by a number of elemental areas including interior and exterior windows. The radiosity-irradiation method (RIM) was also used in this case in order to compute the illumination (irradiation) of each area. Both Wen and Smith [7] and Cucumo et al.[5] also calculated the redistribution of solar energy inside a building's rooms and the room's effective solar absorptance, a concept which was initially introduced by Duffie and Beckman [8]. Trombe et al.[9] proceeded to implement a similar procedure for calculating 'sun patch' location in a complex enclosure including an occupant. The procedure was implemented in a zone thermal simulation model within the TRNSYS simulation program basically focusing on the thermal comfort of the occupant. The importance of the highest achievable accuracy in solar radiation distribution usually becomes evident inside highly-glazed spaces i.e. greenhouses, sunspaces etc. Mottard and Fissore[10], showed that the view factor weighted approach is not sufficient for highly glazed spaces, from which a large portion of the incoming solar radiation finally escapes. In these configurations, insolation and shading become increasingly important as shown by Pieters and Deltour [11], who used a semi one-dimensional climate model to investigate the relative importance of the constructional parameters that influence the solar energy collecting efficiency of greenhouses under Western European conditions. Increased computational effort is needed in the approach of Hiller et al. [12], who developed an algorithm for shading and insolation calculations focusing mainly on

surface shapes, interactions and shading, but including the effects of internal non-opaque surfaces.

The improved accuracy of the previous methodologies comes at the cost of computational complexity and effort. It is interesting to note that another commercial software targeting building thermal simulation (EnergyPlus [13]) includes both a simpler form of view factor weighted methodology and a more complex beam tracking one as options.

The purpose of this paper is to present a simple and computationally efficient methodology that distributes the total incoming solar radiation in enclosures of parallelepiped shape, taking into account enclosure geometry, view factor theory and the position of the sun throughout the day. The total incoming solar radiation from multiple openings is distributed among the enclosure surfaces with the use of simple distribution factors, without the need to separately trace each opening's beam radiation incidence on other surfaces. Analytical expressions are used for the view factors in parallelepiped geometry, this being the most common representative geometry in the majority of buildings: i.e. a typical building consists of surfaces that are either perpendicular or parallel. In order for the algorithm to be tested and verified, it was linked to the commercial simulation software *TRNSYS* and the results were compared to the absorptance-weighted area ratio distribution algorithm [3] that the software already uses. As previously mentioned, more accurate distribution algorithms including multiple and/or specular reflections may be applied but the motivation for the present methodology is a) to provide improved accuracy and physical basis compared to the

absorptance weighted area ratio method, b) to include geometrical characteristics of the enclosure walls and openings such as area, relative position and distance, c) to account for the incident solar radiation on each of the multiple openings, as a function of geographical location of the building and the opening's orientation relative to the diurnally varying position of the sun and d) to retain simplicity in form, implementation and computational effort.

In the next section, the proposed numerical methodology is described, followed by information concerning the test case building configuration and the whole simulation process. Results and comparison of the two approaches are presented for two different simplified building models and finally, findings and conclusions regarding implementation of the proposed algorithm are provided.

2. Numerical methodology

2.1 Overview

The purpose of this section is to describe the mathematical expressions that form the basis of the distribution algorithm and yield the solar energy balances through the use of time varying distribution functions. The distribution functions represent the fraction of the total incoming direct solar radiation that reaches each of the enclosure's surfaces. As a result, the sum of all values of these functions is not allowed to exceed unity (1) within a zone at any moment in time. The algorithm applies to any enclosure (zone) that consists of six opaque surfaces, having from one to five external openings (windows or doors), one on each surface. If more than one opening is present on a given surface, then they are considered as a single opening of area equal to the total area of the openings.

The methodology will be applied as an extension to the commercial thermal simulation software TRNSYS [3], which will be responsible for calculating incident solar radiation on external surfaces, distribution of the diffuse and reflected components and performing the thermal balances on the walls of the enclosure.

Solar energy is commonly considered through its direct and diffuse components. One of the major simplifications assumed here is that, after passing through an opening, direct solar radiation loses most of its directional character and is emitted diffusely towards all other surfaces of the enclosure. The assumption is that of a uniform diffuse transmitter, the same as that considered in TRNSYS [3], and has been empirically found acceptable for the common cases of shaded, diffusing or multi-layered glazings ([14]). Another popular thermal simulation software (EnergyPlus [13]) also assumes all incident direct solar radiation to be transmitted as diffuse, if the glass is diffusing or a window shade is in place. For clear, unshaded glass, there is a portion of the direct solar radiation component that will create a ‘solar patch’ on the opposing internal surface but this would necessitate more complex geometrical calculations involving the exact position of the sun and the openings’ borders (see for example [9]). If each wall is considered as a single surface (as is the case here) then even if solar patches were calculated, the absorbed heat flux would be distributed over the whole surface thus damping the details of the sun patch position. This is actually the practice in the advanced option in Energy Plus [13] where sun patches are calculated.

Data regarding the errors induced by the assumption that solar radiation is diffusely transmitted by complex glazing is difficult to find. An indication of the effects can be

derived from the work presented by Wall ([2]) for an enclosure with an attached sunspace, where four different distribution algorithms were used. The differences in the distribution algorithms involved both the diffuse and/or specular transmittance and the view factor or area weighted assumptions. For winter calculations, the differences among the models in absorbed, transmitted and escaping radiation were small i.e. a maximum of 15% but for summer calculations, they reached 50%. For the enclosures being studied here, where the glazed areas are a small fraction of the enclosure, the errors induced by the assumption of diffuse behavior are expected to be much smaller since the percentage of solar radiation re-escaping through the glazing will be negligible.

Furthermore, it should be kept in mind that, although isotropic diffuse solar radiation enters equally distributed through all of the enclosure's external openings, the direct component will strike each opening as prescribed by the diurnally varying position of the sun. This information is retained in the present calculation procedure and it is combined with the relative geometrical position of each opening and the remaining internal surfaces. Therefore, the direct solar radiation component that is transmitted through each opening still retains a significant degree of directional character. This is the major improvement over the absorptance weighted area ratio method, against which comparison will be performed.

The methodology is applied only for the direct component; the diffuse component is distributed according to absorptance-weighted area ratios and this is also the method used for distributing all radiation after the first reflection from a solid wall since most

building materials can be treated as a Lambert surface: i.e. a perfect uniform and diffuse emitter, absorber and reflector of radiant energy. This assumption is not far from reality since for non-metallic surfaces 75% of the radiant energy is uniformly emitted, i.e. perfectly diffuse, within the cone angle $<60^\circ$ and 97% of the radiant energy is emitted within the cone angle $<80^\circ$ ([15]). Verseghy and Munro ([16]) experimentally determined that neglecting specular reflections in shortwave radiation leads to errors in incident radiation on enclosure surfaces of less than $5\text{-}10\text{ W/m}^2$ (a maximum of 1% for solar radiation values up to 1000 W/m^2), except in enclosures such as greenhouses or atria, which have glazing on over 20% of the enclosure area.

The solar radiation attributed to each internal surface is introduced into the thermal energy balance for the internal walls by the TRNSYS software, and this is where the direct and diffuse components are finally combined.

2.2 View factor calculation

In general, the view factor between two objects can be described as the fraction of the total radiation that leaves the first object and strikes the second. The approaches for the calculation of view factors range between complex numerical methods ([9]) and simple solutions that refer to specific geometries. In the present paper the analytical expressions for view factors between parallel or perpendicular rectangular surfaces, given by Howell and Siegel [17], were used:

$$F_{1 \rightarrow 2} = \frac{1}{(x_2 - x_1)(y_2 - y_1)} \sum_{i=1}^2 \sum_{k=1}^2 \sum_{j=1}^2 \sum_{l=1}^2 \left[(-1)^{(i+j+k+l)} G(x_i, y_j, \eta_k, \xi_l) \right] \quad (1)$$

where:

$$G(x, y, \xi, \eta) = \frac{1}{2\pi} \left\{ \begin{aligned} &(y - \eta)(x^2 + \xi^2)^{1/2} \tan^{-1} \left[\frac{(y - \eta)}{(x^2 + \xi^2)^{1/2}} \right] \\ & - \frac{1}{4} [x^2 + \xi^2 - (y - \eta)^2] \ln [x^2 + \xi^2 + (y - \eta)^2] \end{aligned} \right\} \quad (2)$$

for perpendicular surfaces and

$$G(x, y, \xi, \eta) = \frac{1}{2\pi} \left(\begin{aligned} &(y - \eta) [(x - \xi)^2 + z^2]^{1/2} \tan^{-1} \left\{ \frac{y - \eta}{[(x - \xi)^2 + z^2]^{1/2}} \right\} \\ & + (x - \xi) [(y - \eta)^2 + z^2]^{1/2} \tan^{-1} \left\{ \frac{x - \xi}{[(y - \eta)^2 + z^2]^{1/2}} \right\} \\ & - \frac{z^2}{2} \ln [(x - \xi)^2 + (y - \eta)^2 + z^2] \end{aligned} \right) \quad (3)$$

for parallel surfaces. Equation (1) consists of 16 terms, which are functions of the x,y coordinates of the centers and corners of two rectangular, perpendicular (2) or parallel (3) surfaces respectively. The notation in (1), (2) and (3) is given in Figure 1a, b. There are no limitations concerning the dimensions and the distance between the two surfaces (A_1, A_2), as long as the planes that contain them form a 90° angle in the first case and 0° angle in the second.

2.3 Absorptance-weighted area ratios calculation

Although the approach being presented is general in nature, since it will be implemented using TRNSYS, a short description of the method against which it will be compared is appropriate. According to the TRNSYS manual [3], the incoming diffuse solar radiation and reflected direct solar radiation is distributed within an enclosure with

the use of absorptance-weighted area ratios. Diffuse or reflected direct solar radiation leaving any surface is absorbed by any other surface (s) according to the fraction:

$$f_{d,s,s} = \frac{\alpha_s A_s}{\sum_{\text{surfaces}} (1 - \rho_{d,s}) A_s} \quad (4)$$

where α_s is the solar absorptance of the surface (defined in the building description), A_s is the surface area and $\rho_{d,s}$ stands for the reflectance for diffuse solar radiation of the surface. For opaque surfaces with no transmittance ($\tau_s = 0$):

$$\rho_{d,s} = (1 - \alpha_s) \quad (5)$$

For windows, the transmission losses are considered by:

$$\tau_s = 1 - \alpha_s - \rho_{d,s} \quad (6)$$

For direct solar radiation passing through an external opening, TRNSYS calculates its distribution on the remaining internal surfaces in the same way as for the diffuse component.

From (4)-(6), it is obvious that the only factors that can affect the absorptance-weighted area ratios within a zone are surface material properties and surface area. An opening's relative position with regard to other internal surfaces and its orientation relative to the

diurnally varying position of the sun are neglected. As a result, the solar radiation distribution functions of each surface are always constant in time.

2.4 GS distribution parameters calculation

The proposed methodology modifies the above mentioned procedure for incoming solar radiation by altering the distribution method for the direct component. As commonly assumed ([7], [9]), the reflected components are considered to be diffuse due to the diffuse behaviour of building materials and so, along with their diffuse counterparts, they are still distributed based on the absorptance weighted area ratios. For clarity, the expressions will be presented for a parallelepiped with two windows, each on a different surface. Extension to the situation with windows on all surfaces is straightforward.

The total amount of incoming direct solar radiation, through window 1 ($Q_{dir,1}$), is distributed among the remaining five internal surfaces according to view factor theory ($F_{i \rightarrow j}$ is the view factor from surface i to surface j), as follows:

$$Q_{dir,1} = F_{1 \rightarrow 2}Q_{dir,1} + F_{1 \rightarrow 3}Q_{dir,1} + F_{1 \rightarrow 4}Q_{dir,1} + F_{1 \rightarrow 5}Q_{dir,1} + F_{1 \rightarrow 6}Q_{dir,1} \quad (7)$$

with each term on the right representing the fraction of solar radiation that enters through window 1 and arrives at the corresponding other surface. The energy balance for the direct solar radiation coming through the second window ($Q_{dir,2}$) is:

$$Q_{dir,2} = F_{2 \rightarrow 1}Q_{dir,2} + F_{2 \rightarrow 3}Q_{dir,2} + F_{2 \rightarrow 4}Q_{dir,2} + F_{2 \rightarrow 5}Q_{dir,2} + F_{2 \rightarrow 6}Q_{dir,2} \quad (8)$$

If the total direct radiation entering the enclosure is defined as:

$$Q_{\text{dir,tot}} = \sum_{j=1}^6 GS_j (Q_{\text{dir},1} + Q_{\text{dir},2}) \quad (9)$$

where GS_j is the distribution parameter for surface j (corresponds to the GEOSURF parameter in TRNSYS) then:

$$Q_{\text{dir,tot}} = Q_{\text{dir},1} + Q_{\text{dir},2} \Rightarrow \sum_{i=2..6} F_{1 \rightarrow i} Q_{\text{dir},1} + \sum_{i=1,3..6} F_{2 \rightarrow i} Q_{\text{dir},2} = \sum_{j=1}^6 GS_j (Q_{\text{dir},1} + Q_{\text{dir},2}) \quad (10)$$

and each term ($GS_j (Q_{\text{dir},1} + Q_{\text{dir},2})$) in the last sum of (10) is the energy arriving at surface j . From the left hand side of (10), the energy arriving at surface j is ($F_{1 \rightarrow j} Q_{\text{dir},1} + F_{2 \rightarrow j} Q_{\text{dir},2}$) and the calculation of the distribution parameter GS_j of surface j , for example, is given by :

$$GS_j = \frac{F_{1 \rightarrow j} Q_{\text{dir},1} + F_{2 \rightarrow j} Q_{\text{dir},2}}{Q_{\text{dir},1} + Q_{\text{dir},2}} \quad (11)$$

As a result, (11) gives a factor that's responsible for the distribution of the total incoming direct solar radiation, as a function of relative position of each opening (through the view factors). Furthermore, opening orientation is taken into account since $Q_{\text{dir},1}$ and $Q_{\text{dir},2}$ could, for example, be the incoming radiation from a southern and western window respectively and thus change depending on solar time and latitude. The solar radiation hitting the surface of an internal wall (j) is therefore simply:

$$Q_{\text{dir},j} = GS_j \cdot Q_{\text{dir,tot}} \quad (12)$$

where ($Q_{dir,tot}$) is the sum of direct solar radiation entering from all openings.

3. Simulation

Before describing the models and conditions that were used for the simulation, it is essential to give an outline of the whole process. The flow chart presented in Figure 2 shows the steps that were taken in order for the view factor based distribution of direct solar radiation to be compared with the area ratio distribution method that TRNSYS uses. During the first simulation, the weather data of three different cities, in combination with the geometrical and constructional details of a single-zone and a dual-zone model were used with the TRNSYS software. In this case, the absorptance weighted area ratios method is applied in order to distribute the incoming solar radiation to all the internal surfaces of the zones. The data taken from each simulation step were the total solar radiation absorbed by each surface in [kJ/hr], the incident solar radiation on each opening in [kJ/hr], the temperature of each internal surface in [°C] and the thermal loads arising for each zone.

A calculation algorithm, developed in FORTRAN computer language, used the external distribution of the solar radiation on the openings (calculated from an initial run), a geometrical description of each zone, including its windows and the methodology described in §2.4, in order to produce a file containing the GS parameters for each simulation time step. The above mentioned parameters were inserted, via a data reader, to the TRNSYS software as distribution parameters and a second simulation was then performed. After obtaining the same type of results from the second simulation, comparisons were made and conclusions were drawn. The procedure was applied to a

single-zone and a dual-zone building, using three different weather data files. It should be noted that the second simulation is only necessary if the present algorithm is to be maintained independent. It could be written as an integral part of the TRNSYS software in order to calculate the distribution parameters during each time step of the initial simulation.

Comparisons with other methodologies would require more detailed alterations to the basic thermal simulation code and escape the scope of the present effort. Thus the standard method used in TRNSYS is considered adequate for demonstration of the differences in the calculated results when using the present methodology. Furthermore, this can be considered as a comparison against current standard practice since, as already mentioned, the standard methodology used in TRNSYS is very close to the basic option in EnergyPlus [13].

3.1 Description of Building Models

For the whole simulation process to be completed, two geometrical models were used (Figure 3, 4). The first simulation model refers to a single-zone building of parallelepiped shape, with its front wall facing the south and having two external windows centrally placed on its south and east walls. The building is 3 meters high, 5 meters wide and 10 meters long. As far as its openings are concerned, the dimensions of the south window are 4.00m \times 1.50m (height) and of the east window 2.00m \times 1.50m (height). For economy of space, only the second, dual zone building model is shown in Figure 3 and 4; the first, single zone building is essentially the southern zone (zone 2) without the western window.

The second model is a dual-zone building, with openings on each of its external walls, excluding the ceiling. Figure 3 shows a three dimensional drawing of the model and Figure 4 presents a top view diagram with all the dimensions needed. Both the first and second model are orientated on a north-south axis and their openings are centrally placed on each zone's walls. In the first simulation, the single zone model was used and the dual-zone model was used in the second and third simulation. The difference between the last two simulations is that the internal wall of the building initially has a U-value of $3.14\text{W/m}^2\text{K}$, consisting of two layers of plaster (thickness: 0.025 m, thermal capacity: 1 kJ/kg K and density: 2000 kg/m^3) and one of bricks (thickness: 0.10 m, thermal capacity: 1 kJ/kg K and density: 1800 kg/m^3) and during the last simulation the same wall is considered as a mass wall, consisting of one 0.60 m layer of heavy reinforced concrete, having a U-value of $2.26\text{W/m}^2\text{K}$, thermal capacity of 0.84 kJ/kg K and density equal to 2400 kg/m^3 . This leads to a thermal capacity ratio of ~5 between the two walls.

3.2 Conditions and process

In both buildings, the windows consist of double glazing, with a 10mm air space between them, having a U-value of $2.83\text{W/m}^2\text{K}$. In addition, natural ventilation is considered equal to 2.2ach/h. Initial conditions inside both structures are considered to be $20\text{ }^\circ\text{C}$ and 50% relative humidity. The first building is almost insensitive to outer conditions by applying highly insulated external walls with a U-value of $0.045\text{W/m}^2\text{K}$. In order to study only the incoming solar radiation that's distributed among the inside surfaces, there are no HVAC systems, which leads to a varying internal zone

temperature, and the internal gains from people, lighting, equipment etc. are considered to be zero. The dual zone building is normally insulated; with external walls having a U-value of $0.595\text{W/m}^2\text{K}$. The heating thermostat is set to $22\text{ }^\circ\text{C}$ and the cooling thermostat to $26\text{ }^\circ\text{C}$ and no internal gains, other than solar, are taken into account.

In order to test the methodology in different climates, the simulations were repeated for weather data concerning the cities of Athens (Greece), Helsinki (Finland) and Teheran (Iran). In each case the thermal loads of the building and the percentage of the total incoming solar radiation, absorbed by each wall, were calculated. The results were initially obtained using the area ratio distribution method and then the view factor distribution method was applied. Because of the great number of simulation time steps ($dt=1$ hour, 8760 hours in one year), two representative winter and summer time periods for each year are presented for comparison. The first one from the 33rd until the 41st simulation time step and referring to the 2nd day of January, while the other lasting from the 3654th until the 3668th simulation time step and referring to the 2nd day of June. To be more specific, on January 2nd the sun rises at 7:41am and sets at 5:17pm (local time), but due to TRNSYS round off errors, the first and last time steps to show any energy values are 8:00-9:00am and 4:00-5:00pm. These are the time values shown for winter in Figures 5, 6, 7. The solar azimuth (γ) and the maximum solar altitude (a) angles were analytically calculated (Duffie and Beckman [8]) for the city of Athens during both days of the simulations. For the 2nd of January the solar azimuth angle for sunrise/sunset (γ_{wi}) is 60.55° while the maximum solar altitude (a_{wi}) is 29.49° . For the 2nd of June $\gamma_{sum}=118.61^\circ$ and $a_{sum}=74.72^\circ$.

4. Results and findings

The results for the single zone building are shown in Figure 5. At this point it is essential to stress that Q_{area} refers to the distribution of incoming solar radiation using the area ratio method and $Q_{\text{v.f.}}$ refers to the current view factor based distribution method. The total amount of incoming solar radiation is equal in both cases, because the same solar radiation calculation algorithm (the one provided by TRNSYS) is used. The only difference is the way that this amount is being distributed among the zone surfaces. During the whole day the diffuse part of the total solar radiation that enters the zone through the openings is distributed among all internal surfaces. The direct component of solar radiation will be non-zero only if the sun's position is such to permit incidence on the external surface of the opening. Then the GS factors will lead to a direct solar radiation component being calculated in addition to the diffuse component. This explains the time variation of the $Q_{\text{v.f.}}$ distribution results as opposed to the area distribution method which is based solely on geometrical characteristics, invariable in time.

The structure is the fully insulated parallelepiped and the weather data refer to the city of Athens, Greece. Apart from the floor, the north wall has a constantly greater percentage of absorbed solar radiation mainly because of its position across the south window and its greater surface area, compared to that of the south wall which includes a window. The Q_{area} distribution yields a steady percentage of 9.8% for the south and 16.3% for the north walls during both summer and winter simulation periods. On the other hand, results that come from the $Q_{\text{v.f.}}$ distribution method are diurnally and annually variable. In the winter, the north wall and the floor and roof (not shown due to

symmetry with the floor) absorb more of the incoming solar radiation than that calculated by the area ratio method and this difference becomes greater during the mid-day hours. The physical explanation is that the sun is low in the horizon during the winter ($a_{wi}=29.49^\circ$) and will reach maximum penetration into the zone during the midday hours when it is due south (the orientation of the major zone opening). Since the solar azimuth angle at sunrise and sunset is $\gamma_{wi}=60.55^\circ$, there is minimal direct solar radiation incident on the openings and so it is the diffuse component that determines the radiation distribution at these times of the day. This component is calculated in the same way (area weighted ratios) for both methodologies and therefore, early and late in the day, the same values are calculated for both methods. During midday, the east, west and south walls will absorb less solar radiation than the north wall, the floor and the roof, clearly due to the direct solar radiation component that dominates incident radiation on the south window.

In the summer, the variations for both the north and the south walls are smaller, 16.3-16.8% and 9.3-10% respectively. The higher values at the beginning of the day are due to the direct radiation coming from the east window while the absence of a west window leads to the lower afternoon values. This is also evident from the higher value of absorbed radiation on the southern wall during the first part of the day, when the sun is still low and in the east ($\gamma_{sum}=-118.61^\circ$). According to the solar path during summer ($a_{sum}=74.72^\circ$), the direct component on the southern window is expected to be minimal at midday and this is reflected in the relatively small variation in the north wall's absorbed radiation. The radiation absorbed on the ceiling (not shown) is the same as that of the floor due to the symmetric placement of the openings on the walls and it is

interesting to note that these two surfaces receive the major part of the incoming radiation (28.8%), at midday in winter and during the morning in summer. Because of its large surface area, the floor absorbs the greatest part of the diffuse solar radiation entering the zone (weighted area ratio method) and because of the high view factor values (0.336 between south window and floor and 0.314 between east window and floor), over 30% of the direct solar radiation that comes from the windows reaches the floor (view factor distribution parameters).

Figure 6 shows results for Zone 1 and Figure 7 for Zone 2 of the dual zone building, again for Athens, Greece. In these figures, the south wall of Zone 1 and the north wall of Zone 2, refer to the two sides of the intermediate wall that separates the building into two zones, as shown in Figure 3 and Figure 4. The direct solar radiation entering both zones from their west windows, which did not exist in the single-zone model, is expected to affect the afternoon absorbed solar radiation, especially in the summer ($\gamma_{\text{sum}}=118.61^\circ$). In Figure 6, the distribution of solar radiation on the north and intermediate (south) walls of Zone 1, almost coincide during the winter, no matter what distribution method is used. This is due to the symmetry of the two walls, the absence of a southern opening and the sun rising and setting at an azimuth angle of $\gamma_{\text{wi}}=\pm 60.55^\circ$, so the effect of the diffuse solar radiation component is dominant. The only exception is near the end of the day when there is some direct solar incidence on the larger surface area of the west window. This cannot be reproduced in the weighted area ratio method since solar geometry is not taken into account. During the summer, the effects are more prominent because of the wider sun path ($\gamma_{\text{sum}}=\pm 118.61^\circ$) causing more direct incidence on the east and west windows. Again, it is the floor and ceiling that gather most of the

incoming solar radiation with the view factor distribution method predicting a 5% increase in the summer early morning and late evening, as compared to the weighted area ratio method. Because of the small view factor values between the east and west walls and their opposing openings, the fraction of total solar radiation being absorbed by them is reduced by as much as 20% when compared to the absorptance weighted area ratio distribution method. During winter, the $Q_{v.f.}$ curves are almost of the same shape for these walls but during the summer, when there is more direct solar radiation reaching the east and west openings, there is a larger reduction for the east wall in the early morning and for the west wall in the late afternoon.

Figure 7 refers to Zone 2 which is geometrically similar to simulation model 1 except that Zone 2 has a west facing opening. In Figure 7, the general distribution is the same as in Figure 5 except that in the afternoon, the west facing opening directly affects the results, especially during the summer, when the azimuth angle at sunset is further to the west and the direct solar radiation component is incident on the western and eastern walls for a longer time. The southern window has the biggest surface area, among the other openings of the zone, thus resulting in the intermediate (north-boundary) wall absorbing the second greatest percentage of solar radiation (17-18.5%), as shown in Figure 7. Between the Q_{area} and $Q_{v.f.}$ curves and referring to the intermediate (north) wall, there is a noticeable variation due to the solar path, most prominent in the winter.

For further comparison, surface temperatures and thermal loads were also calculated during simulation, when using both the area ratio and the view factor distribution methods. The maximum temperature variation between any two surface temperatures,

for the whole simulation process was 0.1°C . As far as the thermal loads are concerned, Tables 1 and 2 show the annual values in kWh for both zones of simulation model 2, under different climate conditions. A positive value means heating load and negative stands for cooling loads. It is important to underline that two calculations have been performed: for the first (Table 1), the internal wall has a U-value of $3.14 \text{ W/m}^2\text{K}$ and consists of two layers of plaster and one of bricks while for the second case the same wall is considered as a mass wall, made of one layer of heavy reinforced concrete, which gives a U-value of $2.26 \text{ W/m}^2\text{K}$

Beginning with load variations between both solar radiation distribution methods, they are small and range from 1 to 10 kWh throughout the year. As expected and because of its geographic position, Helsinki exhibits the maximum annual heating load compared to the other cities and has almost no cooling load. Comparison of Table 1 and Table 2 shows that the construction of a mass wall, as a boundary for the two zones, results in an increase of the annual heating loads and a corresponding decrease of the cooling load for Zone 1, with the opposite happening for Zone 2. The above are a direct consequence of the mass wall's ability to store heat because of its large specific heat capacity 7.92 [kJ/h m K] . The solar gains are greater in Zone 2, thus allowing the mass wall's south side to store more heat than the north side throughout the day. Similar observations regarding the importance of thermal mass and direct solar radiation distribution were noted by Yohanis and Norton [1]. As the sun sets, the air temperature inside the zone drops, so the stored heat is released. During winter this process leads to the reduction of the heating load needed by the zone but during the summer it results in an increase of

the cooling load. When the wall's mass is less (Table 1), Zone 1 also benefits from the solar gains of Zone 2 and the heating loads are slightly smaller.

5. Conclusions

The purpose of this study is the development of a method that distributes the total direct solar radiation entering through multiple openings of a building, among its internal surfaces, based on view factor theory. For its effectiveness to be tested, the method was compared with the standard absorptance weighted area ratio distribution method, used by the TRNSYS software. Comparison was performed based on inner surface solar energy absorption and thermal loads for a single and dual zone building as well as for various climate conditions. Results showed that of all parameters, solar radiation absorption by internal surfaces is the one being affected the most by the choice of the solar radiation distribution method. The view factor based method introduces a distribution function dependent upon the building geometry and each opening's orientation relative to the temporally varying sun position. This leads to a time dependent distribution of the direct solar radiation component incident on each opening and the method can be applied for multiple (1-5) openings. For the conventional building models that were used, the variation in the absorbed radiation by an internal wall ranged between 0% and 2% of the total solar radiation entering the zone. In some cases, this corresponds to a variation of 20% of the total radiation being absorbed by the specific surface. Although surface temperatures and thermal loads do not seem to be significantly affected by the use of the view factor based distribution method, its sound physical basis and the relatively small extra computational effort justify its use.

NOMENCLATURE

Latin symbols

A_s	area of surface s , m^2
a	solar altitude angle, deg
$F_{i \rightarrow j}$	view factor for surfaces i and j
$f_{d,s,s}$	fraction of diffuse or reflected solar radiation leaving any surface s and absorbed by any other surface s
$G(x,y,\xi,\eta)$	view factor parameter in eq. 2,3
GS_i	fractions of the total incoming solar radiation absorbed by surface i
Q	solar radiation W/m^2
Q_{th}	thermal load kWh
U	thermal transmittance W/m^2K
x_i	coordinate i on x axis
y_i	coordinate i on y axis
z	distance between 2 parallel rectangular surfaces

Greek symbols

α_s	solar absorptance of surface s
γ	solar azimuth angle, deg
η_i	alternative Cartesian coordinate used in Figure 1
ξ_i	alternative Cartesian coordinate used in Figure 1
ρ	solar reflectance
τ	solar transmittance

Subscripts

area	result obtained by using the absorptance weighted area ratio method for the distribution of total incoming direct solar radiation
d	diffuse solar radiation
dir	direct solar radiation
s	surface
sum	summer day (June 2 nd)
tot	total
v.f.	result obtained by using the view factor method for the distribution of total incoming direct solar radiation
wi	winter day (January 2 nd)

ACCEPTED MANUSCRIPT

REFERENCES

-
- 1 Yohanis Y. G. and Norton B. (2002) Useful solar heat gains in multi-zone non-domestic buildings as a function of orientation and thermal time constant. *Renewable Energy* **27**, 87-95.
 - 2 Wall M. (1997) Distribution of solar radiation in glazed spaces and adjacent buildings. A comparison of simulation programs. *Energy and Buildings* **26**, 129-135.
 - 3 TRNSYS 16 (2005) A TRaNsient SYstem Simulation program. Volume 6: Multizone Building modeling with Type 56 and TRNBuild, Solar Energy Laboratory, Univ. of Wisconsin-Madison, TRANSSOLAR Energietechnik GmbH, CSTB – Centre Scientifique et Technique du Bâtiment, TESS – Thermal Energy Systems Specialists
 - 4 Athienitis A. K. and Stylianou M. (1991) Method and global relationship for estimation of transmitted solar energy distribution in passive solar rooms. *Energy Sources* **13**, 319-336.
 - 5 Cucumo M., Kaliakatsos D. and Marinelli V. (1995) Estimating effective solar absorptances in rooms. *Energy and Buildings* **23**, 117-120.
 - 6 Sparrow E. M. and Cess R. D. (1978) *Radiation Heat Transfer*, Hemisphere, Washington.
 - 7 Wen, J. and Smith, T.F. (2001) Development and Validation of a Dynamic Simulation Model for Thermal Response of a Building. Presented at 8th *International Conference on Building Envelopes*.
 - 8 Duffie J. A. and Beckman W. A. (1991) *Solar Engineering of Thermal Processes*, 2nd Edition, Wiley publications, UK
 - 9 Trombe A., Serres L. and Moisson M. (1999) Solar radiation modelling in a complex enclosure. *Solar Energy* **67**, 297-307.
 - 10 Mottard J. M., Fissore A. (2007) Thermal simulation of an attached sunspace and its experimental validation. *Solar Energy* **81**, 305-315.

-
- 11 Pieters J. G. and Deltour J.M. (1999) Modelling solar energy input in greenhouses. *Solar Energy* 67, 119-130.
- 12 Hiller M.D., Beckman W.A. and Mitchell J.W. (2000) TRNSHED – a program for shading and insolation calculations. *Building and Environment* 35, 633-644
- 13 EnergyPlus, Engineering Reference, The Reference to EnergyPlus Calculations (2007), University of Illinois, Ernest Orlando Lawrence Berkeley National Lab. and U.S. D.O.E. (www.eere.energy.gov/buildings/energyplus)
- 14 ASHRAE (2001), Fundamentals Handbook, ASHRAE.
- 15 Mbiok A., Weber R. (1999). *Radiation in Enclosures*. Springer-Verlag.
- 16 Versegny, D. L. and Munro, D. S. (1989). Sensitivity Studies on the Calculation of the Radiation Balance of Urban Surfaces: I. Shortwave Radiation. *Boundary-Layer Meteorol.* 46, 343-365
- 17 Howell J. R. and Siegel R. (2001) *Thermal Radiation Heat Transfer*, 4th Ed, Taylor and Francis, New York.

FIGURE CAPTIONS

Figure. 1 Schematic diagram of perpendicular (a) and parallel (b) rectangular surfaces

Figure. 2 Flow diagram of the whole simulation process

Figure. 3 Schematic diagram of dual-zone building (*simulation model 2*)

Figure. 4 Top view of dual-zone building (*simulation model 2*)

Figure. 5 Absorbed solar energy percentages of all internal walls (*simulation model 1*)

Figure. 6 Absorbed solar energy percentages of all internal walls (*simulation model 2, Zone 1*)

Figure. 7 Absorbed solar energy percentages of all internal walls (*simulation model 2, Zone 2*)

ACCEPTED MANUSCRIPT

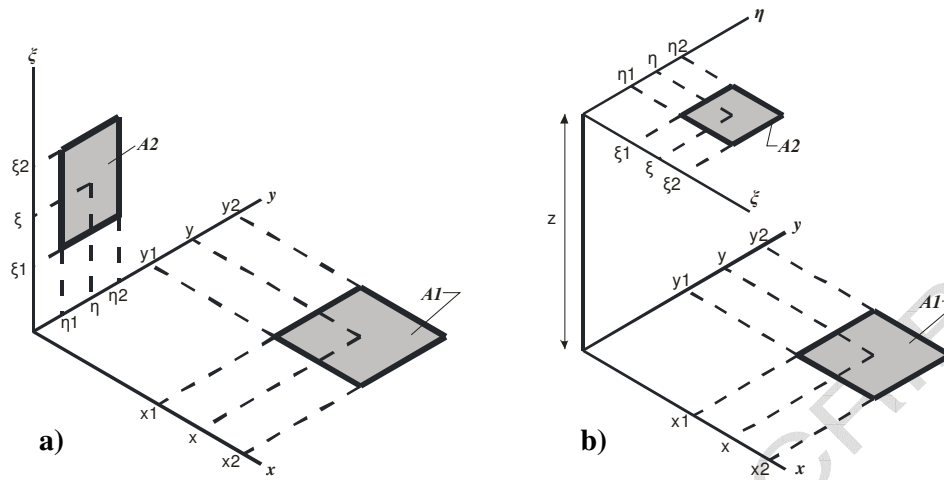


Figure 1 Schematic diagram of perpendicular (a) and parallel (b) rectangular surfaces

ACCEPTED MANUSCRIPT

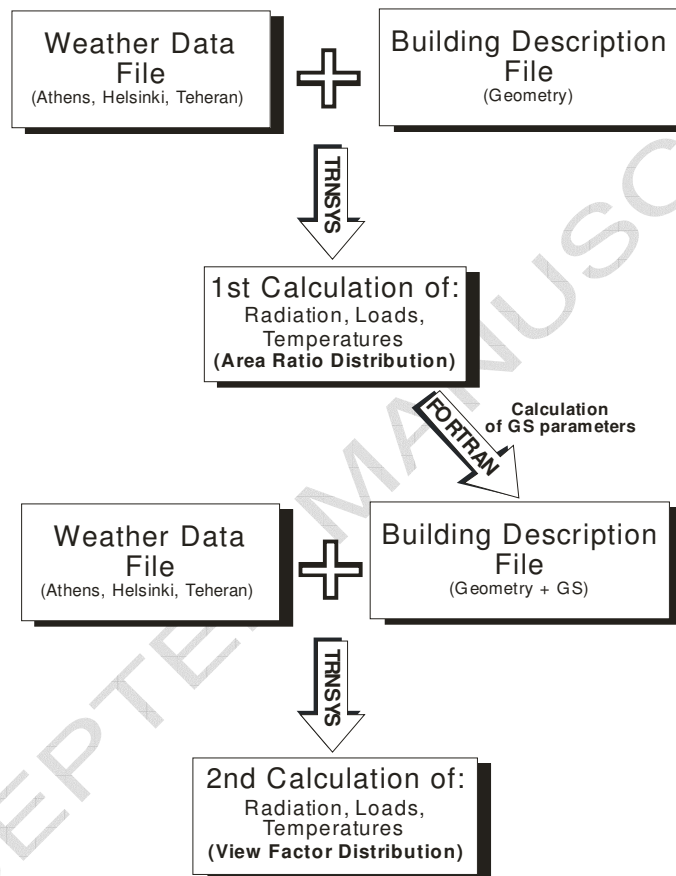


Figure 2 Flow diagram of the whole simulation process

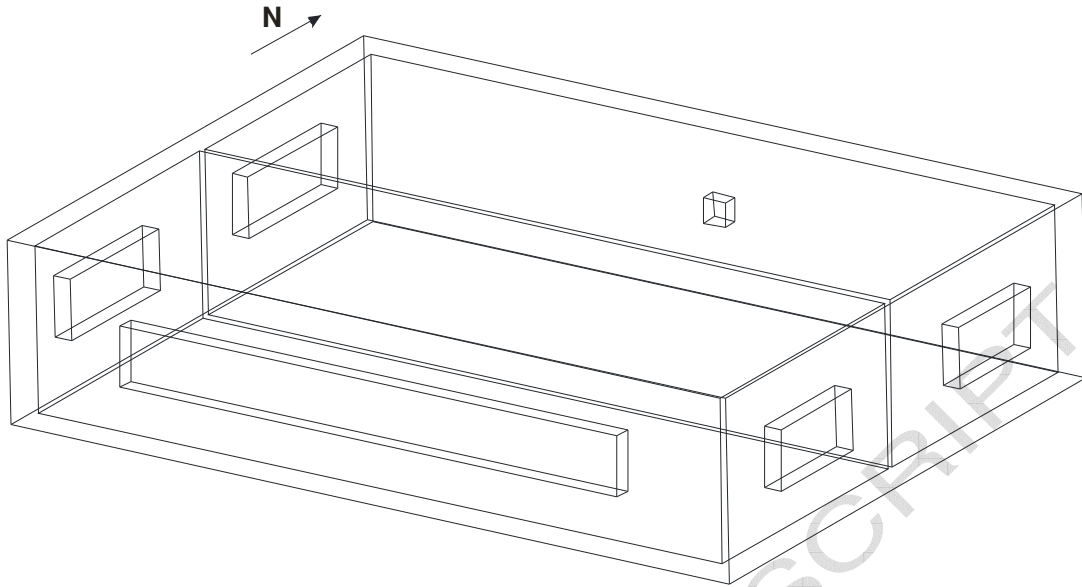


Figure 3 Schematic diagram of dual-zone building (*simulation model 2*)

ACCEPTED MANUSCRIPT

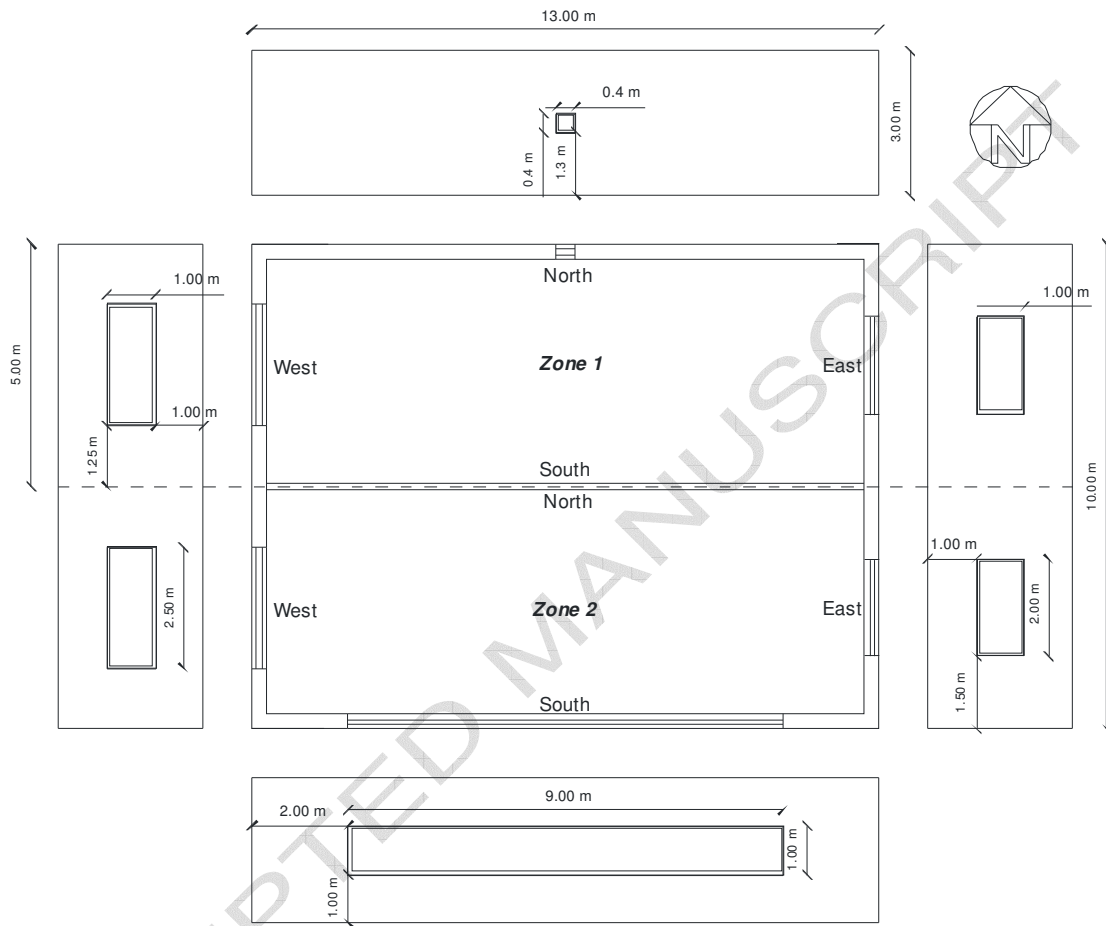


Figure 4 Top view of dual-zone building (*simulation model 2*)

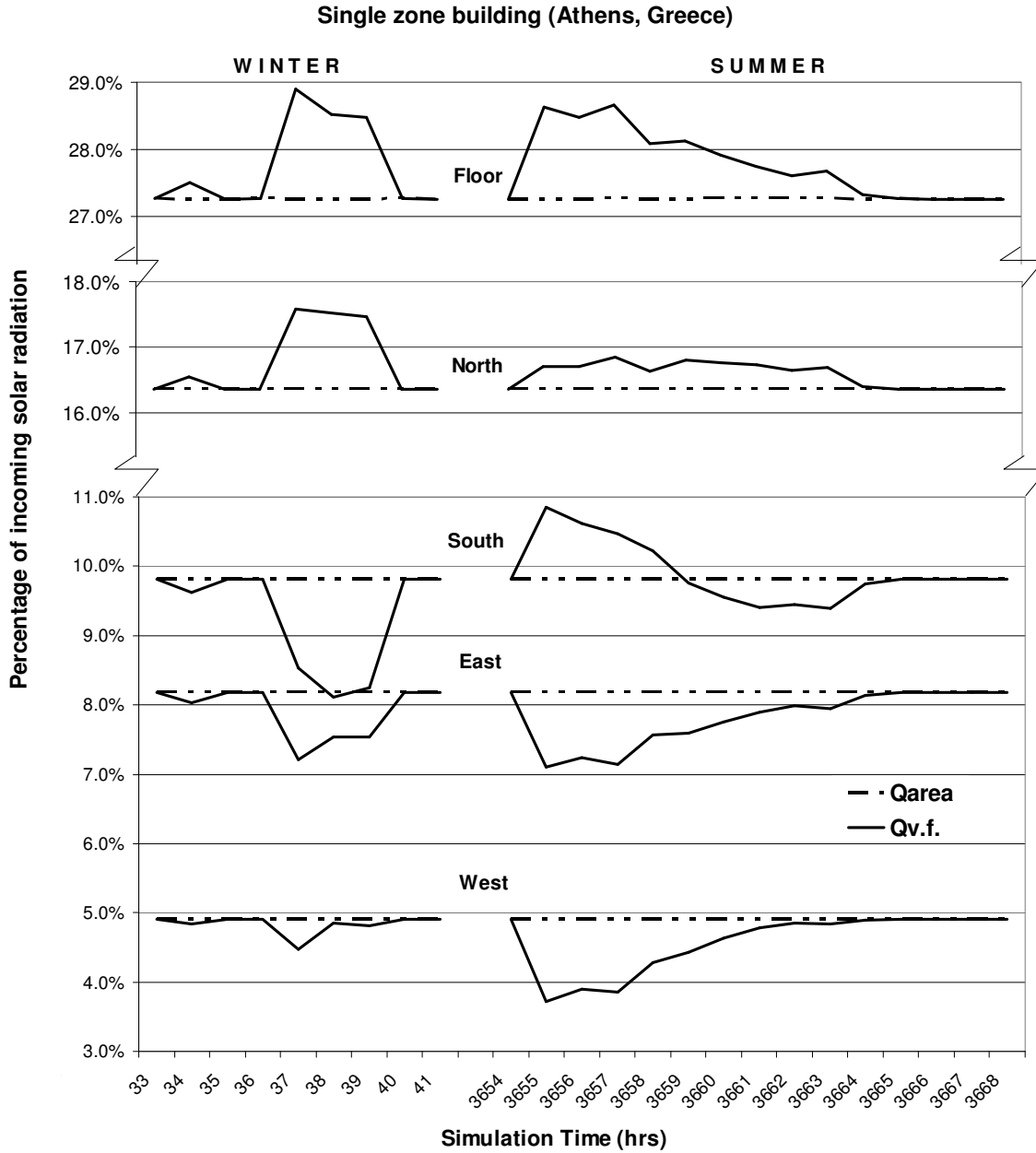


Figure 5 Absorbed solar energy percentages of all internal walls (*simulation model 1*)

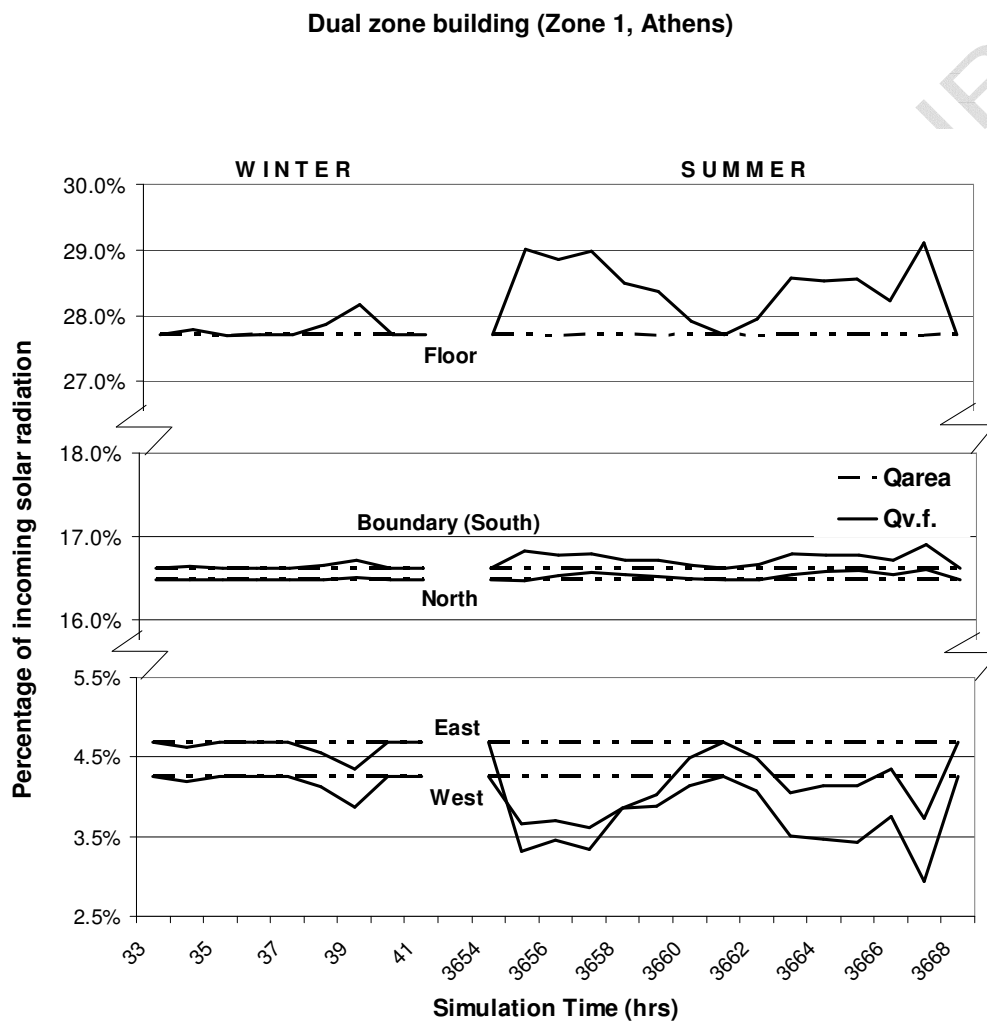


Figure 6 Absorbed solar energy percentages of all internal walls (*simulation model 2, Zone 1*)

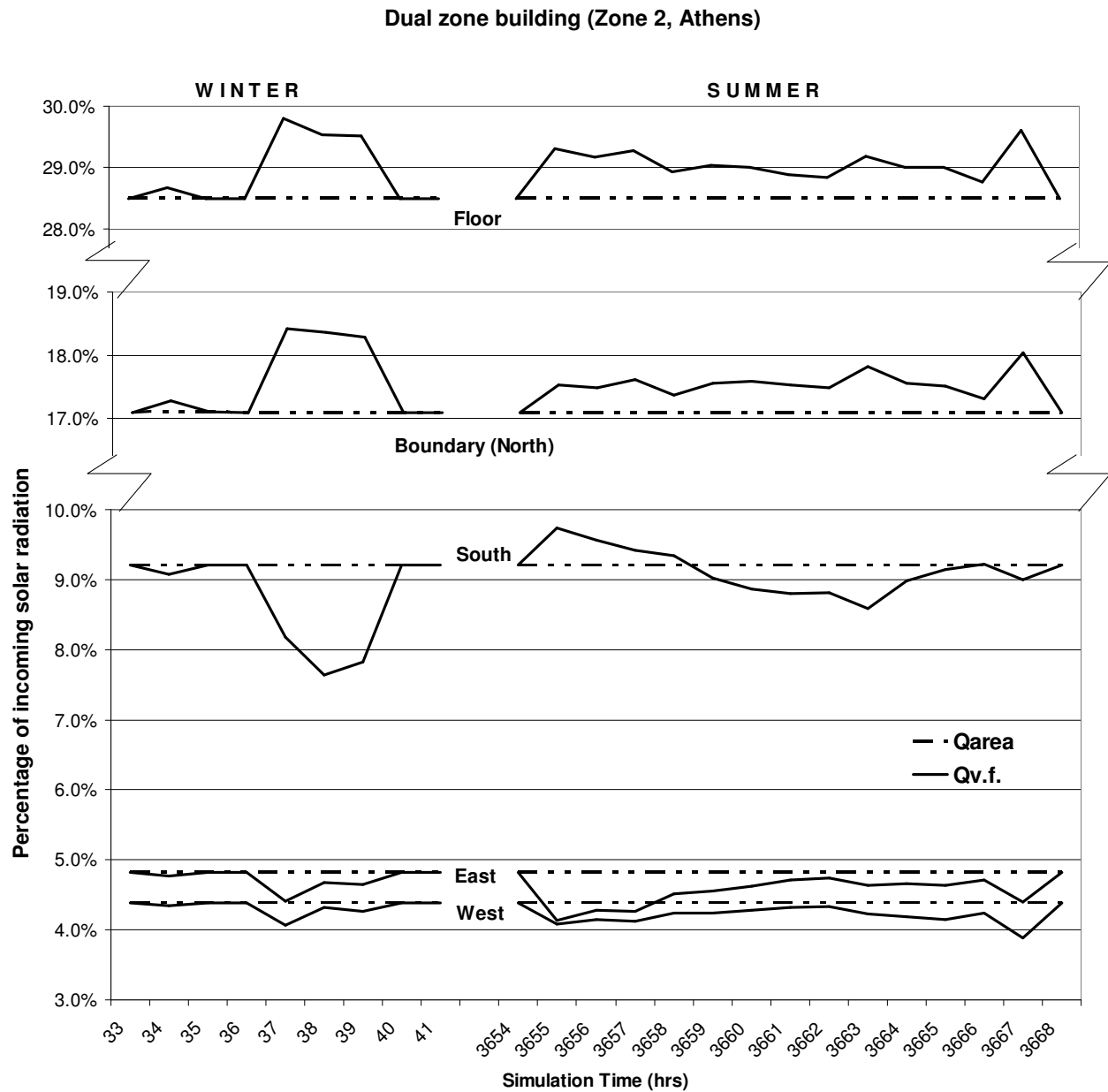


Figure 7 Absorbed solar energy percentages of all internal walls (*simulation model 2, Zone 2*)

	Athens				Helsinki				Teheran			
	Zone 1		Zone 2		Zone 1		Zone 2		Zone 1		Zone 2	
	$Q_{th,area}$	$Q_{th,v.f.}$	$Q_{th,area}$	$Q_{th,v.f.}$	$Q_{th,area}$	$Q_{th,v.f.}$	$Q_{th,area}$	$Q_{th,v.f.}$	$Q_{th,area}$	$Q_{th,v.f.}$	$Q_{th,area}$	$Q_{th,v.f.}$
Jan.	2083	2080	1849	1842	4907	4906	5034	5032	3109	3105	2859	2849
Feb.	1751	1748	1552	1546	4420	4418	4413	4408	2416	2412	2177	2169
Mar.	1541	1538	1384	1380	4021	4017	3874	3865	1725	1721	1502	1494
Apr.	776.9	774.2	650.7	647.1	2799	2796	2589	2583	616.2	613.1	498.7	494
May	161.2	159.7	83.5	80.9	1603	1598	1393	1385	-40.5	-42.1	-116.1	-118.8
June	-247.6	-249.3	-382.5	-386	693.5	689.5	541.6	536.4	-725.3	-728.1	-871.5	-876.8
July	-642.9	-644.9	-845.6	-849.1	458.2	454.3	313.5	308.7	-1253	-1256	-1447	-1453
Aug.	-578.1	-581.8	-847.9	-855.5	833.5	829	661.1	654.9	-1022	-1026	-1289	-1297
Sep.	-126.1	-128.3	-337.6	-346	1809	1805	1689	1682	-319.9	-323.5	-605	-615.4
Oct.	445.1	440.8	298.1	292.3	2787	2784	2712	2704	415.3	410.3	172.5	163.5
Nov.	1190	1187	985.2	979.6	3642	3640	3735	3731	1611	1605	1281	1271
Dec.	1800	1797	1615	1609	4533	4531	4675	4672	2737	2733	2470	2460

Table 1. Annual thermal loads in kWh, for *simulation model 2* with simple internal wall (+ heating, - cooling)

	<u>Athens</u>				<u>Helsinki</u>				<u>Teheran</u>			
	Zone 1		Zone 2		Zone 1		Zone 2		Zone 1		Zone 2	
	$Q_{th,area}$	$Q_{th,v.f.}$	$Q_{th,area}$	$Q_{th,v.f.}$	$Q_{th,area}$	$Q_{th,v.f.}$	$Q_{th,area}$	$Q_{th,v.f.}$	$Q_{th,area}$	$Q_{th,v.f.}$	$Q_{th,area}$	$Q_{th,v.f.}$
Jan.	2101	2098	1848	1840	4902	4902	5038	5036	3126	3123	2854	2844
Feb.	1758	1756	1542	1535	4424	4423	4415	4410	2429	2426	2170	2161
Mar.	1553	1551	1377	1373	4029	4026	3868	3859	1736	1734	1491	1483
Apr.	783.7	781.3	635.8	631.6	2808	2805	2579	2569	622.8	620.3	484.7	480.1
May	171	169.9	85.4	83.2	1622	1618	1388	1379	-27.5	-29.4	-113.2	-116.4
June	-237.2	-238.5	-383.3	-386.6	702.7	699.1	526.3	520.6	-716.9	-719.5	-877.3	-882.8
July	-631.3	-633.4	-851.2	-855.8	466.8	463.4	294.3	288.9	-1244	-1246	-1457	-1463
Aug.	-566.5	-569.1	-859.1	-866	841.6	837.9	641.2	634.6	-1014	-1017	-1307	-1315
Sep.	-124.2	-125.7	-353.6	-361.5	1810	1807	1673	1665	-312.2	-315	-622.5	-633.4
Oct.	437.5	433.7	271.27	265.33	2789	2786	2706	2698	412.1	407.9	148.8	138.9
Nov.	1199	1197	971.8	965.5	3636	3634	3735	3731	1620	1615	1255	1243
Dec.	1808	1806	1606	1599	4526	4525	4678	4674	2749	2745	2459	2448

Table 2. Annual thermal loads in kWh, for *simulation model 2* with internal mass wall

(+ heating, - cooling)